A TEMPLATE MATCHING APPROACH FOR SEGMENTING MICROSCOPY IMAGES

Cheng Chen[1]*, Wei Wang*[1]*, John A. Ozolek*[3]*, Nuno Lages*[4]*, Steven J. Altschuler*[4]
Lani F. Wu[4]*, Gustavo K. Rohde*[1,2]
Center for Bioimage Informatics, Department of Biomedical Engineering[1]
Department of Electrical and Computer Engineering[2]
Carnegie Mellon University, Pittsburgh, PA. 15213
Department of Pathology, Children's Hospital of Pittsburgh, Pittsburgh, PA, 15224[3]
Department of Pharmacology, UT Southwestern Medical Center, Dallas, TX, 75390[4]

ABSTRACT

We describe a generic method for segmenting microscopy images based on supervised statistical modeling. The idea is to utilize example input segmentations to learn a statistical model of the shape and texture of the structures to be segmented. Segmentation of a test image then can be performed by maximizing the normalized cross correlation between the model and neighborhoods in the test image, followed by a final adjustment that utilizes nonrigid registration. We demonstrate the application of the method in segmenting several types of microscopy images of cells and nuclei.

Index Terms— Template matching, normalized cross-correlation, non-rigid registration, N-D image segmentation

1. INTRODUCTION

Image segmentation is an important task in biomedical imaging field. New microscopic imaging modalities often pose difficult segmentation problems which, as experience shows, require extensive fine tuning of existing, or the development of completely anew, segmentation methods. Among a variety of segmentation tasks, one important category is that of segmenting structures which have shapes that can be reasonably well modeled by linear models such as principal component analysis (PCA). Key examples include segmenting nuclei and some types of cells [1], which usually have elliptical-type shapes. Here we utilize a PCA-based method for estimating a mean template and most likely variations in shape for creating a template from user inputed data. Segmentation of a subsequent testing image is then performed by searching for the model instance that best fit local regions in the test image. This idea is not new and has been utilized in several applications. In human brain MR segmentation, for example, anatomical brain atlases have been utilized to segment MR-image via deformable registration [2]. In [3], a shape prior is incorporated into the interactive graph cut approach to mitigate the problems for segmenting the cases where there are diffuse edges, or multiple similar objects in close proximity to one another. Other similar works include that of Lee and Street, [4], and Saddi et al [5], for example. In [6] we described such a procedure focused on segmenting nuclei from fluorescence and several types of histopathology images. The method consisted of a supervised learning procedure for estimating a statistical model, and utilized a normalized cross correlation-based (NCC) registration procedure to search for the model parameters that best fit local regions in an image. We expand the idea to work on different types of data, with a generalization to a multi-channel implementation.

The remaining of this paper is organized as follows: in section 2, we will describe our approach in detail. In section 3, we will apply our approach to different types of data and provide quantitative comparison for validation. In section 4 we offer concluding remarks and discussion.

2. METHODS

Our method is divided into a training procedure, where a statistical model for the shape and texture for the structures to be segmented is built, and a matching procedure that can segment a given test image (Figure 1).

2.1. Training: estimating a statistical model

The training stage consists of creating a template model by learning the shape variations, as well as mean texture, from a set of sample images. Each sample image is required to contain a single structure of interest (such as a single nucleus or cell). Sample images can be produced in many ways. In this work we utilize a simple graphical user interface to enable an expert to manually delineate rectangular image sub-windows each containing only one nucleus from an image of the modality he or she wishes to segment (Figure. 1 top left). For optimal results, the set of sub-windows is recommended to contain varied types and shapes (small, large, bent, irregular shaped, etc.).

Given N such rectangular sub-windows of different sizes, all sub-windows are rigidly aligned by a procedure described in earlier work [7]. In this case, we choose the multi-channel

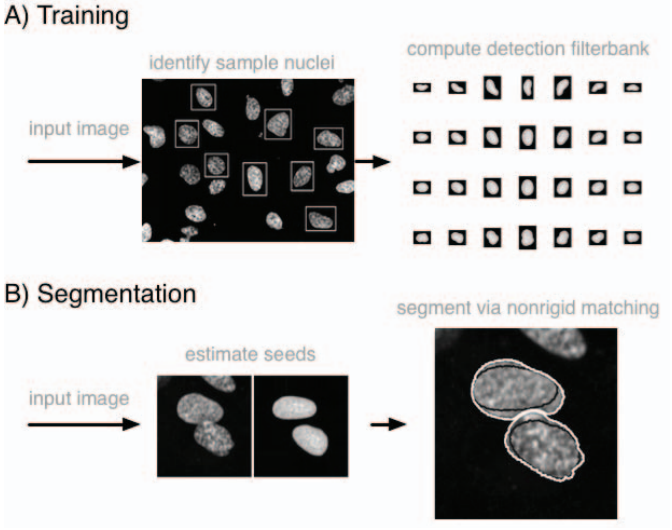


Fig. 1. Overview of our segmentation system. (A) A statistical model is built (from user annotated data) and sampled to comprise a detection filter bank. (B) Subsequent images are then segmented by first finding the model instance (filter) that best matches each region in a whole input image. The best matches are then used as seeds, and are non rigidly aligned to the local region in the input image for accurate border segmentation. The right most figure shows a sub window where two seeds were detected (black contour). The white contour shows the final segmented image (after nonrigid matching).

(in case of color images for example) normalized cross correlation (NCC) as the optimization criterion and include coordinate inversions (image flips) in the optimization procedure. After the rigid alignment, we denote these N rigidly aligned sub-windows as $I_1, \cdots, I_N$ from now on, and use them to estimate a template that will represent an "average" shape as well as texture for this set. Several procedures could be used for this purpose. In this work we choose the procedure outlined in Heitz et al. [8]. The procedure depends on the computation of a nonrigid map that aligns two sample images I_i, and I_j, via $I_i(f_i(\mathbf{x})) \approx I_j(\mathbf{x})$, with $\mathbf{x}$ an input coordinate in the image grid Ω, and $f_i(\mathbf{x}) : \Omega \rightarrow \mathcal{R}^2$. In our work, we designed a non-rigid registration algorithm to achieve this goal. Let $T(\mathbf{x})$ and $S(\mathbf{x})$ be the two images to be matched, the nonrigid registration algorithm aims to find a warping map $u(\mathbf{x})$ that satisfies $T(\mathbf{x}) \approx S_u(\mathbf{x}) = S(\mathbf{x} - u(\mathbf{x}))$ via maximizing the square of the multi-channel NCC cost function:

$$\Phi(u) = \frac{1}{N_{\text{ch}}} \sum_{j=1}^{N_{\text{ch}}} \left(\frac{\langle S_u^j, T^j \rangle}{\|S_u^j\|^2 \|T^j\|^2} \right)^2 \qquad (1)$$

where N_{ch} is the number of channel and $\|T\|^2 = \langle T, T \rangle = \sum_{\mathbf{x}} T(\mathbf{x}) T(\mathbf{x})$. In this work, equation (1) is maximized via steepest gradient ascent.

With an image randomly chosen from the set in the beginning (denoted as $I_0^k(\mathbf{x})$), the template estimation procedure starts iteratively with $k = 1$:

1. Non-rigidly register I_0^k to each training image $I_i, i = 1, 2, ..., N$ such that $I_i(f_i(\mathbf{x})) \approx I_0^k(\mathbf{x})$.
2. Calculate a temporary average shape template $\Psi^k(\mathbf{x}) = I_0^k(\bar{f}^{-1}(\mathbf{x}))$, with $\bar{f} = \frac{1}{N} \sum_{i=1}^{N} f_i$, where f^{-1} is the inverse of the transformation function f.
3. Compute the average texture on the same average shape template above by first registering each sample image in the set to $\Psi^k(\mathbf{x})$ (i.e. $I_i(f_i'(\mathbf{x})) \approx \Psi^k(\mathbf{x})$), and update the template via $I_0^{k+1}(\mathbf{x}) = \frac{1}{N} \sum_{i=1}^{N} I_i(f_i{}'(\mathbf{x}))$.
4. Compute error $= \|I_0^{k+1} - I_0^k\|^2$ (sum of squared errors). If error $< \epsilon$ stops, otherwise set $k = k + 1$ and go back to step 1.

The end result is an image that represents an average template (both in the sense of shape and texture), as well as a set of spatial transformations $f_i (i = 1, ..., N)$ that map each sub-window image to the average template via $I_i(f_i(\mathbf{x})) \approx I_0(\mathbf{x}), i = 1, \cdots N$. We note that in case the input images have multiple channels (e.g. color images), the procedure above is evaluated for all channels simultaneously, and the average texture will also be an average multi channel image.

We next use the PCA technique to derive a statistical model for the possible variations in the shape of the samples. Each spatial transformation can be encoded as a vector of displacements via $\mathbf{v}_i = [f_i(\mathbf{x}_1), ..., f_i(\mathbf{x}_L)]^T$, with L the number of pixels in each image. Thus, we can calculate the mean $\bar{\mathbf{v}}$ and the covariance $\mathbf{C}$ of the set of spatial displacements $\mathbf{v}_1, \cdots, \mathbf{v}_N$. Using the PCA technique, the principal deformation modes are given by the eigenvectors $\mathbf{q}_p, p = 1, 2, 3, ...$ of the covariance matrix $\mathbf{C}$ satisfying $\mathbf{C}\mathbf{q}_p = \lambda_p \mathbf{q}_p$. A statistical model for the shape variations can be obtained by retaining the top eigenvalues and eigenvectors covering 95% (this percentage chosen arbitrarily) of the variance in the dataset. The model can be evaluated by choosing an eigenvector and calculating $\mathbf{v}_{p,b_p} = \bar{\mathbf{v}} + b_p \mathbf{q}_\mathbf{p}$. The corresponding template is obtained by re-assembling $\mathbf{v}_{p,b_p}$ into a corresponding spatial transformation f_{p,b_p}, and computing $I_0(f_{p,b_p}(\mathbf{x}))$. We evaluate the model with b_p from $-5\sqrt{\lambda_p}$ to $5\sqrt{\lambda_p}$ in intervals of $\sqrt{\lambda_p}$ and generate a set of simulated template images representing likely shape deformations. In addition, we augment the set of simulated template images by including rotations (6 in our implementation) as well as variations in size (2 in our implementation). Figure 1 (top right) contains a few examples images generated in this way from a nuclei sample dataset. Here, we name the set of simulated template images as the "detection filter bank" for the segmentation use in the next subsection.

In addition, for each simulated template image, a binary mask that delineates the biological structure of interest inside will be produced. Instead of hand segmenting all simulated template images, we only segment the average template image by manually providing an initial contour and refining the contour utilizing a level set approach [9].

2.2. Testing: detection and segmentation

The testing stage consists of two steps: (1) detect the structures of interest and obtain an approximate segmentation for an given input image and (2) perform accurate segmentation via nonrigid multi-channel image matching. The whole process is based on the idea of maximizing the multi-channel NCC between the statistical model for a given dataset and local regions in an input image.

In the first detection step, we calculate the multi-channel NCC of the input image (denoted $J^i(\mathbf{x})$, with $i = 1 \cdots N_{\text{ch}}$ in case of multichannel images) against each filter $W_p^j(\mathbf{x})$, $p = 1, \cdots, K$ in the detection filter bank, and get the response at the pixel $\mathbf{u}$, for example, as:

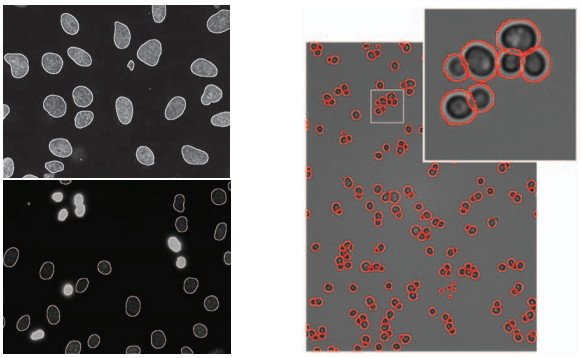
$$\gamma_p(\mathbf{u}) = \frac{1}{N_{\text{ch}}} \sum_{j=1}^{N_{\text{ch}}} \frac{\sum_{\mathbf{x}} J^j(\mathbf{x}) W_p^j(\mathbf{x}-\mathbf{u})}{\bar{J}^j(\mathbf{u}) \bar{W}_p^j}. \qquad (2)$$

with $\bar{J}^j(\mathbf{u})$ being the sum of squared values of the j^{th} channel of image J under the template positioned at $\mathbf{u}$, and $\bar{W}_p^j$ the sum of squared values of template p. A detection probability image M can be computed by keeping the maximum response at the pixel $\mathbf{u}$ as: $M(\mathbf{u}) = \max_p \gamma_p(\mathbf{u})$. Potential guesses are identified by finding the pixel locations in M which are greater than a threshold μ. In addition, multiple detections are ensured not to be too close to each other. To that end, the thresholded detection image M is searched for its highest response, then the second highest which is at least a distance r from the first, the third highest which are at least distance r from the previous two, and so on. The process is repeated until all pixels in the thresholded detection image M have been investigated. We note that each detected pixel in M also has its associated best match from the detection filter bank. Consequently, the output provides not only the locations of biological structures (such as nuclei) that we are looking for, but also a rough guess for its shape from the binary mask of its best matching template (see bottom middle of Figure 1).

Then, in the second segmentation stage, for each biological structure of interest detected, our algorithm provides a spatially accurate segmentation by non-rigidly registering each approximate guess to the input image using the algorithm described in equation 1.

3. EXPERIMENTAL RESULTS

To validate our proposed approach, we test it on three different datasets. These include: fluorescence microscopy images of nuclei, histopathology microscopy images of nuclei, and brightfield microscopy images of yeast cells. For each experiment, we manually select 20 samples for training. Several parameters are kept constant for all experiments: percent of variance retained in PCA analysis (95%), $\epsilon = 0.04$ for the calculation of the average template, the step size in the gradient ascent procedure $\kappa = 5 \times 10^4$, the scale number in the multi-scale strategy $s = 2$, and the smoothing parameter in the gradient ascent procedure $\sigma = 1.5$ (pixels). The remaining parameters were empirically selected for each dataset.



(a) (b)

Fig. 2. (a) Results on nuclei microscopy images; (b) Result on cellular microscopy image

3.1. 2D grayscale images

First, we test our approach on 2D grayscale microscopy images. The nuclei images (two datasets of U2OS and NIT3T3 cells from Dr. Murphy's group [1]). The U2OS (48 images) and NIH3T3 (49 images) dataset were obtained with the Hoechst 33342 fluorescence signal, and the ground truth is provided by experts [1]. In Figure. 2(a), we show two segmentation results of nuclei (top: U2OS, bottom: NIH3T3) randomly selected. In Figure. 2(b), we show the result of yeast cells, which were observed with bright light under a 40x objective using a Nikon Ti-E2000 microscope. Cells are delimited either by a dark or white boundary.

In addition, we calculate the quantitative results using different evaluation metrics (details are described in [1]) for fluorescence microscopy images of nuclei [1] and compare to the existing popular methods(shown in Table. 1). We can see that our approach is able to provide comparable or even better performance with the existing ones.

3.2. Segmenting color microscopy images

We apply our method to segmenting color microscopy images of nuclei obtained using histopathology techniques. These include the Feulgen stain which highlights DNA only. If no counterstaining is performed then only nuclei are visible demonstrating chromatin patterns as deep magenta hues

Table 1. Quantitative Comparison of Nuclei Segmentation

Algorithm (U2OS/NIH3T3)	Rand Index	Jaccard Index	Hausdorff	NSD ($\times 10$)	Split	Merged	Added	Missing
Otsu Threshold	92%/74%	2.2/2.1	34.9/36.7	1.2/3.5	1.1/0.8	2.4/2.1	0.3/1.7	5.6/26.6
Watershed (direct) [10]	91%/78%	1.9/1.6	34.9/19.3	3.6/3.7	13.8/2.9	1.2/2.4	2.0/11.6	3.0/5.5
Active Masks [11]	87%/72%	2.1/2.0	148.3/98.0	5.5/5.0	10.5/1.9	2.1/1.5	0.4/3.9	10.8/31.1
Our Result	94%/88%	2.5/2.7	95.8/134.1	0.86/2.9	0.0/0.0	2.1/4.0	1.6/3.3	4.3/3.8

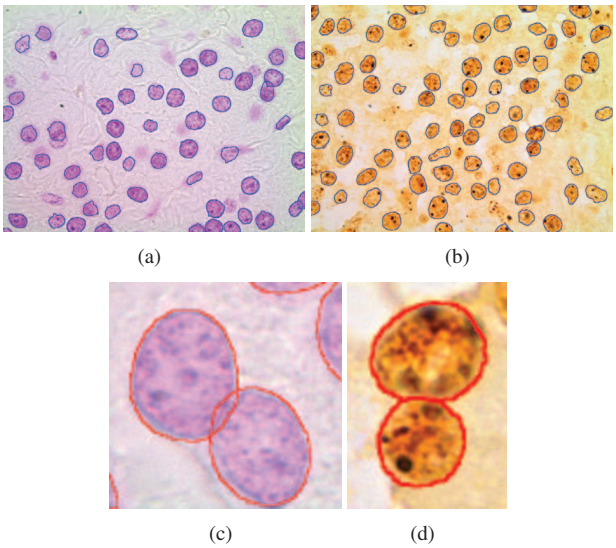


Fig. 3. Results on histopathology nuclei images

shown in Figure 3(a). The second is a silver-based technique that stains the intranuclear nucleolar organizing regions (NORs) (black intranuclear dots) without counterstaining (Figure 3(b)). In addition, we also show the results for overlapping nuclei case (3(c)) and touching nuclei case (3(d)).

4. CONCLUSIONS AND DISCUSSIONS

We described a template matching-based segmentation approach using statistical learning and non-rigid registration techniques. The technique is designed to segment structures whose shape and texture do not vary greatly. If so, the approach can segment images accurately. We analyzed the performance of the method visually on three different datasets. In addition, we compared the performance of the method to several other available methods quantitatively in the task of segmenting nuclei from fluorescence images. Overall, our results show comparable or even better performance. We note that in segmenting yeast cells, the method also segmented other small, non-cell objects. These, however, could be removed from the final segmentation result by eliminating structures which are smaller than a certain threshold. We note that one drawback of our approach is the selection of optimal parameters, and our future work is to investigate how to select the optimal parameters automatically. We are also working on implementing and testing the method with 3D image data.

Acknowledgements

C.C, W.W., and G.K.R. acknowledge support from NIH grant GM088816. LFW was supported by NIH GM081549 and the Welch Foundation I-1619. SJA was supported by NCI R01CA133253 and the Welch Foundation I-1644 (S.J.A.).

5. REFERENCES

[1] L.P. Coelho, A. Shariff, and R.F. Murphy, "Nuclear segmentation in microscope cell images: a hand-segmented dataset and comparison of algorithms," in *Biomedical Imaging: From Nano to Macro, 2009. ISBI'09. IEEE International Symposium on*. IEEE, 2009, pp. 518–521.

[2] M.B. Cuadra, C. Pollo, A. Bardera, O. Cuisenaire, J.G. Villemure, and J.P. Thiran, "Atlas-based segmentation of pathological mr brain images using a model of lesion growth," *Medical Imaging, IEEE Transactions on*, vol. 23, no. 10, pp. 1301–1314, 2004.

[3] D. Freedman and T. Zhang, "Interactive graph cut based segmentation with shape priors," in *Computer Vision and Pattern Recognition, 2005. CVPR 2005. IEEE Computer Society Conference on*. IEEE, 2005, vol. 1, pp. 755–762.

[4] K.M. Lee and W.N. Street, "Model-based detection, segmentation, and classification for image analysis using on-line shape learning," *Machine vision and applications*, vol. 13, no. 4, pp. 222–233, 2003.

[5] K.A. Saddi, C. Chefd'hotel, M. Rousson, and F. Cheriet, "Region-based segmentation via non-rigid template matching," in *Computer Vision, 2007. ICCV 2007. IEEE 11th International Conference on*. IEEE, 2007, pp. 1–7.

[6] C. Cheng, W. Wang, J. A. Ozolek, and G. K. Rohde, "A template matching approach for segmenting cell nuclei from microscopy images," *Medical Imaging, IEEE Transactions on*, in preparation.

[7] G. K. Rohde, A. J. S. Ribeiro, K. N. Dahl, and R. F. Murphy, "Deformation-based nuclear morphometry: capturing nuclear shape variation in hela cells.," *Cytometry A*, vol. 73, no. 4, pp. 341–350, 2008.

[8] G. Heitz, T. Rohlfing, C.R. Maurer Jr, et al., "Statistical shape model generation using nonrigid deformation of a template mesh," in *Proceedings of SPIE Medical Imaging*. Citeseer, 2005, vol. 5747, pp. 1411–1421.

[9] C. Li, C. Xu, C. Gui, and M. D. Fox, "Level set evolution without re-initialization: A new variational formulation," in *Proceedings of IEEE Conference on Computer Vision and Pattern Recognition (CVPR)*, Washington, DC, USA, 2005, vol. 1, pp. 430–436.

[10] C. Wählby, I.M. SINTORN, F. Erlandsson, G. Borgefors, and E. Bengtsson, "Combining intensity, edge and shape information for 2d and 3d segmentation of cell nuclei in tissue sections," *Journal of Microscopy*, vol. 215, no. 1, pp. 67–76, 2004.

[11] G. Srinivasa, M.C. Fickus, Y. Guo, A.D. Linstedt, and J. Kovacevic, "Active mask segmentation of fluorescence microscope images," *IEEE Transactions on Image Processing*, vol. 18, no. 8, pp. 1817–1829, 2009.